

The Crystal Structures of Tin(II) Chloride Dihydrate in High- and Low-Temperature Phases as Studied by Neutron and X-Ray Diffractions

Katsuki KITAHAMA and Hideko KIRIYAMA

The Institute of Scientific and Industrial Research, Osaka University, Yamada-kami, Suita, Osaka 565

(Received June 27, 1977)

The neutron-diffraction results for deuterated single crystals have shown definitely that the phase transition is ascribable to the ordering of the hydrogen atoms. The ordered arrangement below the transition temperature ($T_t = 234$ K) agrees well with the NMR results. No doubling of the unit cell or loss of the center of symmetry can be detected. In the disordered phase above T_t , four deuterons of two non-equivalent water molecules are distributed into seven sites. The occupancy factors of the individual sites have been refined by least-squares methods under different constraints. Bernal and Fowler's ice rule is obeyed in the H-bonded water layers, and the water molecules of crystallization scarcely dissociate at all. The crystal structure has been redetermined by the X-ray diffraction method at 209 and 223 K, using an $\text{SnCl}_2 \cdot 2\text{H}_2\text{O}$ single crystal. No distinct change in the structure of non-hydrogen atoms has been disclosed on passing through the transition point ($T_t = 218$ K). However, in the close vicinity of T_t , the a and c lattice parameters and the three H-bonded $\text{O} \cdots \text{O}$ distances steeply change in association with the ordering of the hydrogen atoms.

Crystals of $\text{SnCl}_2 \cdot 2\text{H}_2\text{O}$ exhibit a phase transition accompanied by a characteristic dielectric anomaly at 218 K (at 234 K for its deuterated analogue).¹⁾ Successive studies of proton (PMR) and deuteron (DMR) magnetic resonance,^{2,3)} X-ray diffraction,⁴⁾ and Raman scattering⁵⁾ have shown that the phase transition should be ascribed to the ordering of hydrogen atoms in H-bonded water layers without another distinct change in the crystal structure. Furthermore, the critical phenomena of the phase transition have been studied by other approaches, such as specific heat,^{6,7)} and dielectric measurements.⁸⁾ On the other hand, the theory of the phase transition⁹⁾ and the explanation of the dielectric behavior¹⁰⁾ have been developed in cooperation with these experiments.

This study was performed to elucidate more directly the hydrogen arrangement in the H-bonded network below and above the phase-transition temperature, T_t . Some of the neutron-diffraction (ND) results have been given previously.¹¹⁾ Additionally, the crystal structures at 209 and 223 K as well as the lattice parameters in the 93–293 K range were determined by X-rays in order to make sure whether or not the hydrogen-ordering is associated with structural changes in other atoms.

Neutron-diffraction Experiments

Samples. Deuterated single crystals, $\text{SnCl}_2 \cdot 2\text{D}_2\text{O}$, were used for the present ND study, because X-ray photographs taken at both 293 and 93 K had shown no change in the crystal structure on deuteration. Single crystals were grown from a deuterated hydrochloric acid solution saturated with anhydrous tin(II) chloride. A large single crystal was cut into three cylindrical pieces, weighing 0.8957, 0.9282, and 1.2361 g. The smallest one has dimensions of 5.5, 6.0, and 7.5 mm along the a , c , and b axes respectively, and it was mainly used. Another crystal, weighing 12.3 g, was also used at the initial stage of the experiment. These four crystals are labeled S1, S2, S3, and S4 in increasing order of weight. Since this compound is sensitive to

moisture, many sorts of organic adhesives, and metals, each single-crystal sample was wrapped with Teflon tape and then placed in an aluminium capsule.

Intensity Data Collection. All the ND measurements were carried out with the KUR-1 reactor of the Research Reactor Institute, Kyoto University. The intensity data of Bragg reflections were collected on a Rigaku neutron four-circle diffractometer at 297 and 88 K. The neutron flux had a density of $7 \times 10^4 \text{ n cm}^{-2} \text{ s}^{-1}$ at the specimen and a wavelength of 0.994 Å. The reflections were measured within $\sin \theta/\lambda$ of 0.72 Å^{-1} . The 2θ - ω step-scan technique was used with the step size of $\Delta 2\theta = 0.1^\circ$. The scan range for each reflection was adjusted so as to include at least five background points on both sides of the peak. The counting time was controlled by monitoring the intensity of an incident neutron beam. A graphical method was used for integrating the observed intensity and for correcting the background. No correction for absorption was made because of the small linear absorption coefficient ($\mu = 0.255 \text{ cm}^{-1}$). The standard intensity was monitored every 25 reflections. There was no significant change in the intensity of the standard reflection throughout the data collection.

At room temperature (297 K) the $hk0$ and $0kl$ intensity data were collected with the biggest crystal, S4, while $0kl$, $h0l$, and hkh were measured with the smallest, S1. For the measurement at 88 K, a ten-liter Dewar vessel containing liquid nitrogen was attached on the ϕ table of the four-circle diffractometer to cool the specimen down to 88 K by a conduction method. Because this arrangement limited the tilting angle of the χ -circle to the range of $-20^\circ < \chi < 20^\circ$, three crystals, S1, S2, and S3, were mounted with b , a , and c axes respectively along the ϕ -axis of the goniostat.

Some forbidden reflections for the $\text{P2}_1/\text{c}$ space group, as determined by X-rays, were carefully checked, but their intensities did not exceed more than one half of the background level. Thus, no evidence was found to suggest that the low-temperature phase is either antiferroelectric or ferroelectric.

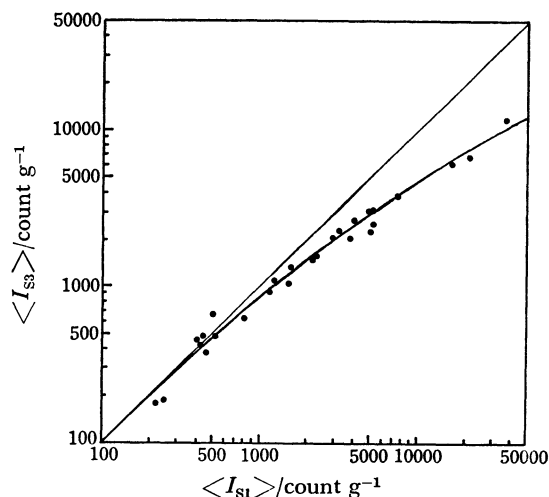


Fig. 1. The extinction effect observed in the ND experiment of $\text{SnCl}_2 \cdot 2\text{D}_2\text{O}$. The reduced intensity of a bigger crystal S3 is plotted against that of a smaller crystal S1, both on logarithm scale. Deviation from the line with a slope of unity reflects the extinction effect.

Extinction Correction. In the early stage of least-squares refinements, it became apparent that the intensities were affected by severe extinction and that the data required adequate corrections. Two kinds of isotropic corrections were attempted, for simplicity neglecting the dependence of the extinction on the Bragg angles. One was an exponential type with a single parameter, such as $I_o = I_c \exp(-kI_c)$. This type of correction was unsuccessful, probably because the I_o/I_c ratio was less than 0.7, as was suggested by Hamilton.¹²⁾ The other was based on the reduced intensity, $\langle I \rangle$, which was a quotient of the observed intensity divided by the crystal weight. The reduced intensity of a bigger crystal, $\langle I_b \rangle$ was plotted against that of a smaller crystal, $\langle I_s \rangle$, both on the logarithm scale. The difference in these reduced intensities, $\Delta \langle I \rangle (= \langle I_s \rangle - \langle I_b \rangle)$, was evaluated from the smoothed curve shown in Fig. 1. Thus, the intensity data were corrected by extrapolating the $\langle I \rangle$ to an infinitesimally small weight, using either of the following two equations:

$$\begin{aligned} \langle I_{\text{corr}} \rangle &= \langle I_b \rangle + \frac{W_b}{W_b - W_s} \Delta \langle I \rangle \\ &= \langle I_s \rangle + \frac{W_s}{W_b - W_s} \Delta \langle I \rangle \end{aligned}$$

where W_b and W_s are the weights of a bigger and a smaller crystal, respectively. This type of correction was effective in avoiding negative temperature factors and in lowering the R -value by more than 2%. However, this correction seemed to be not enough for the biggest crystal, S4; therefore its intensity data were excluded from the final least-squares refinement.

X-Ray-diffraction Experiments

A single crystal of $\text{SnCl}_2 \cdot 2\text{H}_2\text{O}$, with dimensions of $0.08 \times 0.1 \times 0.32 \text{ mm}^3$ and sealed in a Lindemann-glass capillary, was used throughout the X-ray work. This crystal was mounted on a Rigaku four-circle diffracto-

meter, with its c -axis along the ϕ -axis of the goniostat. The crystal was cooled by blowing a stream of cold nitrogen, using an X-ray low-temperature device manufactured by the Rigaku Denki Co. The reflection intensities at 209 and 223 K, and monoclinic cell dimensions (space group; $P2_1/c$) from 93 to 293 K were measured with an Mo $K\alpha$ radiation monochromatized by pyrolytic graphite. The temperatures were controlled within $\pm 0.5 \text{ K}$ during each measurement of the lattice parameters, and within $\pm 1.0 \text{ K}$ throughout each collection of the intensity data. The cell dimensions at a given temperature were refined by a least-squares method using 21 reflections with 2θ between 40 and 65° . They are summarized in Table 1. All the intensity data were collected by means of the 2θ - ω scan technique. No correction was made for absorption ($\mu = 54.9 \text{ cm}^{-1}$).

TABLE 1. LATTICE PARAMETERS AT VARIOUS TEMPERATURES

T/K	$a/\text{\AA}$	$b/\text{\AA}$	$c/\text{\AA}$	$\beta/^\circ$	$V/\text{\AA}^3$
93	9.140(3)	7.150(2)	8.914(4)	114.32(3)	532.5(3)
125	9.153(2)	7.156(2)	8.958(3)	114.35(2)	534.5(2)
153	9.167(3)	7.165(2)	8.961(3)	114.33(2)	536.2(3)
173	9.178(2)	7.172(2)	8.970(3)	114.36(2)	537.9(3)
195	9.200(3)	7.184(2)	8.975(3)	114.44(2)	540.0(3)
209	9.213(2)	7.189(2)	8.969(3)	114.50(2)	540.6(3)
223	9.244(3)	7.202(2)	8.963(3)	114.64(2)	542.6(3)
233	9.262(3)	7.212(2)	8.953(4)	114.73(3)	543.2(4)
243	9.272(3)	7.217(2)	8.949(3)	114.79(2)	543.6(3)
253	9.283(3)	7.227(2)	8.955(4)	114.82(3)	545.3(4)
268	9.299(4)	7.237(3)	8.961(4)	114.89(3)	547.1(4)
293	9.320(8)	7.255(4)	8.970(7)	114.91(5)	550.1(8)

Space group; $P2_1/c$ (throughout the temperature range), $Z=4$, F.W. 225.63 g mol⁻¹, $\rho_{\text{obsd}} = 2.710^{(10)}$, $\rho_{\text{calcd}}(293 \text{ K}) = 2.724 \text{ g cm}^{-3}$, $\mu(\text{Mo } K\alpha) = 54.85 \text{ cm}^{-1}$. E.s.d.'s are given in parentheses.

Structure Analyses and Refinements

Structure at 88 K by Neutron Diffraction. The approximate positions of deuterons were easily determined from the Fourier projections of nuclear-scattering density along the a and c axes; the signs were based on the heavy-atom coordinates from a previous X-ray study.⁴⁾ No evidence was found for any disordering of the deuteron positions. The extinction correction described above was made prior to the refinement. In order to check whether or not the deuterium substitution was complete, the neutron-scattering length of deuteron was refined, as well as the positional and isotropic thermal parameters for all the atoms and a scale factor, in the full-matrix least-squares refinement. The obtained scattering length was $b_D = (0.605 \pm 0.018) \times 10^{-12} \text{ cm}$, indicating that the unsubstituted hydrogen was negligibly small. The scattering lengths used were $b_{\text{Sn}} = 0.610$, $b_{\text{Cl}} = 0.961$, $b_{\text{O}} = 0.577$, and $b_{\text{D}} = 0.612$ in units of 10^{-12} cm from Neutron Diffraction Commission, 1969.¹³⁾

The refinement was performed by a block-diagonal least-squares method with 814 reflections, in which positional and anisotropic thermal parameters for all the atoms, an overall temperature factor, and a scale factor (a total of 65 parameters) were varied until the maximum shift in any parameter was less than one-fourth of its e.s.d. The quantity minimized in this

TABLE 2. OBSERVED AND CALCULATED STRUCTURE AMPLITUDES($10F$) FOR $\text{SnCl}_2 \cdot 2\text{D}_2\text{O}$ AT 88 K BY NEUTRON DIFFRACTION^{a,b)}

H	FO	FC	H	FO	FC	H	FO	FC	H	FO	FC	H	FO	FC	H	FO	FC	H	FO	FC	H	FO	FC	H	FO	FC	H	FO	FC						
K=0	L=0		1	50	-34	2	23	-21	1	3	-2	K=1	L=3		-7	36	36	-2	47	-46	K=4	L=6		-1	62	59	1	3	-7						
1	59	81	2	49	-34	3	15	-13	-12	34	35	-6	57	56	-1	35	-34	-2	56	-51	0	80	-82	0	80	-82	0	80	-82						
2	4	-1	3	68	69	4	0	-1	K=0	L=2		-11	24	27	-5	21	21	0	57	56	-1	19	-17	1	43	-42	K=6	L=9							
3	70	72	4	29	29	5	24	25	-12	16	14	-10	16	-16	-4	75	70	1	9	-10	0	52	47	2	47	50	-1	18	-19						
4	30	-26	5	6	-7	6	24	26	-11	0	0	-9	0	2	-1	35	38	1	16	-16	3	84	-82	0	11	-12									
5	81	-81	6	31	33	7	8	-7	-10	97	-93	-8	9	4	0	6	0	K=4	L=5		5	36	44	K=0	L=10										
6	11	-9	7	51	49	8	13	-13	-9	8	3	-7	64	-60	1	25	26	-2	21	21	K=5	L=6		-10	18	-21	-7	21	-19						
7	38	37							-8	70	65	-6	27	-26	2	40	41	-1	34	34	-2	14	-14	K=1	L=8		-11	18	20						
8	13	-10	K=9	L=0		K=5	L=1		-7	85	-80	-5	56	52	3	13	-7	0	33	32	-1	10	-8	K=1	L=8		-10	61	67						
9	47	-45	1	42	-45	-10	32	-32	-6	18	-16	-1	45	46	4	7	6	1	7	-7	0	53	-51	-12	10	14	-9	7	5						
10	47	47	2	0	0	-9	0	-2	-5	35	32	0	60	-63	5	44	-39	K=5	L=5		1	16	-19	-11	33	-37	-8	104	-104						
11	17	18	3	19	-19	-8	17	18	-4	126	-132	1	9	-8	6	50	-46	K=6	L=6		-9	0	0	-9	0	0	-6	6	-4						
			4	12	-10	-7	22	19	-3	120	-128	2	29	26	7	16	17	-2	47	-46	K=6	L=6		-8	39	-35	-5	117	-116						
K=1	L=0		5	17	17	-6	52	51	-2	36	-28	3	97	-90	8	9	9	-1	17	-9	-7	47	-46	-7	27	37	-4	19	19						
1	13	-11				-1	5	3	4	76	-70	9	48	49	0	87	91	0	87	91	0	6	6	-6	5	11	16	-3	99	102					
2	30	29	K=10	L=0		-4	19	17	0	26	21	5	60	56	2	2	L=4				1	6	-4	-5	14	18	-2	0	5						
3	28	-25	0	48	48	-3	10	9	1	65	72	6	11	12	K=2	L=4				K=6	L=5		-2	22	-19	K=7	L=6		-4	73	73				
4	24	-18	1	9	8	-2	35	-34	2	121	123	7	32	-31	-1	15	-13	-2	22	-19	K=7	L=6		-2	37	39	0	52	49						
5	3	2	2	35	-37	-1	41	-41	3	17	13	8	65	62	0	50	-42	-2	22	-19	K=7	L=6		-2	37	39	0	52	49						
6	15	-11				0	12	-8	4	41	-42	9	53	51	1	19	-17	-1	8	-5	-2	6	6	-2	45	47	1	41	42						
7	49	47	K=1	L=1		1	56	-57	5	29	24	10	43	-47	5	6	-4	0	19	-18	-1	11	-10	-1	35	36	2	0	2						
8	22	23	-12	40	41	2	83	-84	6	45	-47	K=2	L=3		7	55	-50	6	10	6	1	16	-16	0	21	19	0	14	-12						
9	18	-8	-11	5	-2	3	22	-19	7	56	-57	K=2	L=3		7	55	-50	6	10	6	1	16	-16	0	21	19	0	14	-12						
10	2	1	-10	38	-38	4	6	-5	8	7	-7	-1	32	-32	8	11	-11	K=7	L=5		-2	28	-28	2	21	21	-11	24	-26						
11	55	-56	-8	7	-7	6	46	44	10	13	-18	1	4	-6	5	22	23	K=3	L=4		-1	18	-19	-2	31	-29	4	45	49						
K=2	L=0		-7	12	-10	7	88	93	9	22	-23	K=1	L=2		6	0	4	-1	30	-33	1	10	-12	0	56	54	K=2	L=8		-7	10	-11			
0	29	-21	-6	23	20	8	8	9	K=1	L=2		-12	0	6	6	0	0	0	35	31	1	6	-6	K=2	L=8		-6	39	-40						
1	60	-66	-5	36	33	9	22	-23	-11	38	41	8	10	-8	1	5	1	K=8	L=5		-2	34	31	K=1	L=7		0	43	38						
2	88	-102	-4	35	34	K=6	L=1		-10	18	22	9	16	-17	K=4	L=4		-1	31	30	-12	40	42	1	16	15	-3	0	1						
3	17	17	-3	31	30	-9	12	-13	-9	55	58	K=3	L=3		-2	38	-38	0	13	14	-11	17	18	2	42	37	-2	30	31						
4	35	37	0	10	-7	-8	20	-20	-8	0	7	-1	33	33	-1	6	-6	1	43	-46	-10	42	-44	3	8	-11	-1	15	16						
5	87	-105	3	10	10	-7	18	-28	-7	15	-9	0	63	-60	0	29	26	K=9	L=5		-8	84	80	5	59	57	1	8	9						
6	14	-11	4	24	25	-6	10	10	-6	26	29	0	28	26	1	10	-7	-2	57	-57	-7	27	-26	K=3	L=8		-1	10	-11						
7	57	60	5	21	-20	-6	10	10	-6	26	29	0	28	26	1	10	-7	-2	57	-57	-7	27	-26	K=3	L=8		-1	10	-11						
8	45	-43	6	42	40	-5	28	26	-5	11	-7	K=4	L=3		-2	17	-18	K=5	L=4		-1	37	-37	-6	16	-16	K=3	L=8		-1	10	-11			
9	24	22	7	86	79	-4	8	7	0	34	-30	K=4	L=3		-2	17	-18	K=5	L=4		-1	37	-37	-6	16	-16	K=3	L=8		-1	10	-11			
10	69	68	8	19	-18	-3	21	-17	1	16	-18	K=4	L=3		-2	17	-18	K=5	L=4		-1	37	-37	-6	16	-16	K=3	L=8		-1	10	-11			
11	0	-1	9	41	-40	-2	29	-23	2	17	7	-1	6	5	-2	18	-13	0	46	42	-5	42	39	-1	54	-58	K=2	L=10		-2	43	-41			
K=3	L=0		11	11	-10	0	24	-21	4	40	-40	1	14	-15	0	0	3	K=0	L=6		-3	80	-74	1	32	-36	-1	76	-75						
1	16	-15				1	14	15	5	47	-45	K=5	L=3		-2	50	51	K=6	L=4		-10	75	-76	0	14	-14	-1	42	43						
2	49	-55	K=2	L=1		2	53	52	6	56	-53	K=5	L=3		-2	50	51	K=6	L=4		-10	75	-76	0	14	-14	-1	42	43						
3	4	0	-11	18	-18	3	17	19	7	23	20	-2	32	30	-1	32	-30	-2	27	-27	-9	60	-56	1	30	28	0	70	-70						
4	7	-9	-10	29	-29	4	0	-2	8	14	13	-1	38	-39	-1	32	-31	-8	53	-51	2	52	49	1	18	-20	K=3	L=10		-1	9	-8			
5	10	-9	-9	19	-19	5	0	0	9	18	18	0	58	-59	-1	32	-31	-8	53	-51	2	52	49	1	18	-20	K=3	L=10		-1	9	-8			
6	40	37	-8	12	-12	6	11	-12	10	12	16	1	16	-13	0	14	-20	-7	35	-31	3	8	2	4	11	-13	K=5	L=8		0	17	16			
7	18	-15	-7	3	-3	7	11	-11	K=2	L=2		-1	30	27	K=6	L=3		-2	16	-18	K=7	L=4		-4	57	54	6	22	-24	1	27	-35			
8	7	-5	-6	36	19	8	0	-2	K=2	L=2		-1	30	27	K=6	L=3		-2	16	-18	K=7	L=4		-4	57	54	6	22	-24	1	27	-35			
9	16	16	-5	25	24	9	14	11	0	84	-98	-1	31	-31	-2	21	-20	-3	77	75	K=2	L=7		-1	4	1	K=6	L=8		-1	10	7			
10	8	-8	-4	5	5	1	15	7	0	16	-17	0	16	-17	-1	29	-28	-2	68	-65	K=2	L=7		-1	4	1	K=6	L=8		-1	10	7			
11	23	23	-2	35	-33	-8	25	-27	6	0	0	K=7	L=3		-2	56	61	K=8	L=4		2	12	-20	2	11	-11	1	5	2	K=5	L=10		-1	12	15
K=4	L=0		0	21	-18	-7	44	-44	7	22	-17	K=7	L=3		-2	56	61	K=8	L=4		2	12	-20	2	11	-11	1	5	2	K=5	L=10		-1	12	15
0	120	150	1	14	14	-6	36	-35	8	6	-1	K=7	L=3		-2	56	61	K=8	L=4		2	12	-20	2	11	-11	1	5	2	K=5	L=10		-1	12	15
1	14	11	2	44	42	-5	23	-22	9	54	53	-1	35	34	-2	4	2	3	43	42	3	15	-14	4	0	-1	K=7	L=8		0	0	0			
2	28	-28	3	33	32	-4	15	13	10	19	23	0	62	-60	-1	22	21	4	62	59	4	0	-1	5	9	-1	48	-46							
3	79	82	4	15	16	-3	33	31	K=3	L=2		1	11	11	0	25	21	5	7	4	5	9	9	-1	48	-46									
4	15	14	5	0	2	-2	19	17	K=3	L=2		1	11	11	0	25	21	5	7	4	5	9	9	-1	48	-46									
5	36	-35	6	15	-14	-1	10	7	-1	21	23	K=8	L=3		-2	5	6	K=9	L=4		-2	34	-36	K=1	L=6		-1	24	24	-11	21	-25			
6	19	16	7	17	-19	0	23	21	0	48	47	K=8	L=3		-2	5	6	K=9	L=4		-2	34	-36	K=1	L=6		-1	24	24	-11	21	-			

TABLE 3. FINAL POSITIONAL PARAMETERS ($10^4 x_j$) AND THERMAL PARAMETERS ($10^2 B_{ij}/\text{\AA}^2$) IN THE LOW-TEMPERATURE PHASE OF $\text{SnCl}_2 \cdot 2\text{D}_2\text{O}$

Estimated standard deviations are given in parentheses. The anisotropic thermal factors are of the form: $T = \exp[-1/4(h^2 a^{*2} B_{11} + \dots + 2klb^* c^* B_{23})]$.

	<i>x</i>	<i>y</i>	<i>z</i>	<i>B</i> ₁₁	<i>B</i> ₂₂	<i>B</i> ₃₃	<i>B</i> ₁₂	<i>B</i> ₁₃	<i>B</i> ₂₃
Sn	3773 (3)	2565 (4)	5335 (3)	16 (8)	54 (9)	36 (7)	3 (9)	23 (6)	13 (9)
Cl (1)	2830 (2)	4899 (3)	6836 (2)	73 (6)	62 (6)	53 (5)	2 (7)	39 (5)	-6 (6)
Cl (2)	3071 (2)	5008 (3)	3043 (2)	50 (5)	59 (6)	58 (5)	-2 (6)	34 (5)	12 (6)
O (1)	1096 (4)	1685 (5)	4156 (4)	54 (9)	78 (10)	41 (8)	-27 (11)	26 (8)	8 (11)
O (2)	-683 (4)	2058 (5)	5931 (4)	56 (9)	62 (9)	59 (9)	0 (12)	35 (8)	-7 (10)
D (1)	—	—	—	—	—	—	—	—	—
D (2)	1014 (4)	331 (5)	4056 (4)	120 (11)	81 (10)	149 (11)	-9 (12)	82 (9)	-21 (12)
D (3)	—	—	—	—	—	—	—	—	—
D (4)	502 (4)	2004 (6)	4847 (4)	131 (11)	147 (12)	141 (11)	-26 (14)	95 (10)	-10 (13)
D (5)	-117 (5)	2509 (7)	7022 (5)	198 (14)	199 (15)	134 (11)	8 (15)	67 (11)	-39 (14)
D (6)	—	—	—	—	—	—	—	—	—
D (7)	-1550 (5)	2907 (7)	5399 (5)	106 (11)	154 (13)	218 (13)	63 (15)	8 (11)	2 (15)

refinement was $\Sigma w(|F_o| - |F_c|)^2$, with a unit weight for all reflections. The final $R[\Sigma(|F_o| - |F_c|)/\Sigma|F_o|]$ was 0.081 for all reflections and 0.078 for non-zero reflections. The final F_c and F_o , with the extinction corrections, are given in Table 2. The final positional and thermal parameters are listed in Table 3, where the anisotropic temperature factors are shown in \AA^2 for comparison with the isotropic ones at 297 K.

Structure at 297 K by ND. The difference Fourier projections of the nuclear-scattering density along the *a* and *c* axes and [101] direction were calculated

using the heavy-atom positions from the X-ray study.⁴⁾ The maps revealed that the four deuterons scatter in seven sites of the asymmetric unit, providing direct evidence for the disordering of deuteron positions in the high-temperature phase. Moreover, the heights of the deuteron peaks were considerably different from one another. Accordingly, the occupancy factors of the individual deuteron sites should be adjusted as well as the positional and thermal parameters in the least-squares refinement.

A full-matrix least-squares refinement based on 311

TABLE 4. OBSERVED AND CALCULATED STRUCTURE AMPLITUDES ($10^2 F$) FOR $\text{SnCl}_2 \cdot 2\text{D}_2\text{O}$ AT 297 K BY NEUTRON DIFFRACTION^{a, b)}

H	K	L	FO	FC	H	K	L	FO	FC	H	K	L	FO	FC	H	K	L	FO	FC	H	K	L	FO	FC	H	K	L	FO	FC
0	1	1	71	-64	0	5	8	82	-124	-9	0	2	157	171	-5	0	6	60	81	-3	0	12	394	-367	6	4	-6	118	102
0	1	2	223	-169	0	5	9	170	-152	-8	0	2	570	605	-4	0	6	362	366	-2	0	12	112	-121	6	5	-6	0	101
0	1	3	531	-532	0	5	10	0	-21	-7	0	2	438	-447	-3	0	6	526	526	1	1	-1	266	-251	6	6	-6	0	-8
0	1	4	410	-375	0	6	0	295	314	-6	0	2	0	-48	-2	0	6	537	-517	1	2	-1	179	204	6	7	-6	127	-142
0	1	5	800	806	0	6	1	213	-185	-5	0	2	328	319	-1	0	6	379	-347	1	3	-1	146	152	6	8	-6	0	23
0	1	6	98	-101	0	6	2	388	-360	-4	0	2	963	-1141	0	0	6	50	41	1	4	-1	220	-232	7	1	-7	173	-184
0	1	7	136	-132	0	6	3	70	-37	-3	0	2	978	-1207	1	0	6	370	-350	1	5	-1	292	-308	7	2	-7	0	-25
0	1	8	201	-195	0	6	4	109	-141	-2	0	2	366	-327	2	0	6	92	-80	1	6	-1	147	127	7	3	-7	306	-284
0	1	9	152	-161	0	6	5	120	-128	-1	0	2	49	-26	3	0	6	402	334	1	7	-1	108	111	7	4	-7	120	95
0	1	10	102	-91	0	6	6	81	39	0	0	2	183	158	4	0	6	420	387	1	8	-1	107	94	7	5	-7	175	-186
0	1	11	67	48	0	6	7	175	-177	1	0	2	714	746	5	0	6	124	130	1	9	-1	78	-108	7	6	-7	0	-50
0	2	0	307	-270	0	6	8	220	-186	2	0	2	1044	1257	6	0	6	117	164	1	10	-1	52	-59	7	7	-7	88	-126
0	2	1	154	-151	0	6	9	0	3	3	0	2	246	252	7	0	6	411	414	2	1	-2	351	323	8	1	-8	300	328
0	2	2	811	-944	0	7	1	213	248	4	0	2	167	-146	-12	0	8	180	185	2	2	-2	725	822	8	2	-8	330	321
0	2	3	54	-113	0	7	2	179	169	5	0	2	441	414	-11	0	8	129	170	2	3	-2	388	-396	8	3	-8	168	-142
0	2	4	235	-230	0	7	3	438	-426	6	0	2	185	-180	-10	0	8	331	-323	2	4	-2	123	121	8	4	-8	142	161
0	2	5	132	-155	0	7	4	283	303	7	0	2	162	-232	-9	0	8	0	5	2	5	-2	154	190	8	5	-8	87	133
0	2	6	165	234	0	7	5	281	283	8	0	2	170	179	-8	0	8	97	-94	2	6	-2	368	351	8	6	-8	71	110
0	2	7	107	-132	0	7	6	62	73	9	0	2	56	-56	-7	0	8	666	-638	2	7	-2	311	-328	8	7	-8	0	57
0	2	8	229	-229	0	7	7	159	-169	10	0	2	56	32	-6	0	8	134	-142	2	8	-2	205	240	9	1	-9	0	-12
0	2	9	0	17	0	7	8	0	43	11	0	2	0	73	-5	0	8	312	341	2	9	-2	0	-31	9	2	-9	67	-78
0	2	10	157	178	0	8	0	223	256	-13	0	4	0	97	-4	0	8	183	243	2	10	-2	123	130	9	3	-9	141	-148
0	2	11	0	7	0	8	1	105	-99	-12	0	4	260	-280	-3	0	8	0	92	3	1	-3	191	-173	9	4	-9	157	139
0	3	1	461	458	0	8	2	260	-267	-11	0	4	0	-28	-2	0	8	409	404	3	2	-3	125	-171	9	5	-9	68	55
0	3	2	202	181	0	8	3	125	-160	-10	0	4	73	12	-1	0	8	414	363	3	3	-3	519	-534	10	1	-10	50	-76
0	3	3	630	-624	0	8	4	172	185	-9	0	4	177	-175	0	0	8	580	-528	3	4	-3	73	41	10	2	-10	370	390
0	3	4	437	438	0	8	5	86	61	-8	0	4	0	-6	1	0	8	281	-247	3	5	-3	153	-145	10	3	-10	0	25
0	3	5	482	436	0	8	6	247	270	-7	0	4	397	416	2	0	8	168	170	3	6	-3	190	-217	10	4	-10	79	64
0	3	6	55	91	0	8	7	168	149	-6	0	4	773	779	3	0	8	564	-517	3	7	-3	324	-339	8	1	0	75	31
0	3	7	365	-305	0	9	1	152	128	-5	0	4	261	255	4	0	8	260	-266	3	8	-3	40	-70	9	1	0	113	-119
0	3	8	116	157	0	9	2	0	9	-4	0	4	149	141	5	0	8	187	200	3	9	-3	148	-150	7	1	1	475	427
0	3	9	58	71	0	9	3	143	-127	-3	0	4	157	143	-11	0	10	0	-12	4	1	-4	405	-439	8	1	1	87	-152
0	3	10	105	71	0	9	4	60	36	-2	0	4	734	-796	-10	0	10	185	190	4	2	-4	85	106	7	1	2	268	277
0	3	11	271	268	0	9	5	134	113	-1	0	4	457	-463	-9	0	10	47	-40	4	3	-4	299	340	8	1	2	163	136
0	4	0	951	1263	0	10	0	196	225	0	0	4	96	89	-8	0	10	565	-522	4	4	-4	35	82	6	1	3	0	5
0	4	1	78	51	0	10	1	0	-70	1	0	4	0	29	-7	0	10	80	-126	4	5	-4	246	-247	7	1	3	159	-201
0	4	2	190	-201	0	10	2	141	-129	2	0	4	664	601	-6	0	10	133	-152	4	6	-4	66	81	5	1	4	367	-342
0	4	3	99	82	1	0	0	621	803	3	0	4	419	369	-5	0	10	763	-713	4	7	-4	125	141	6	1	4	351	-305
0	4	4	242	254	2	0	0	0	-21	4	0	4	95	138	-4	0	10	57	53	4	8	-4	52	50	4	1	5	48	-42
0	4	5	224	211	3	0	0	658	681	5	0	4	374	362	-3	0	10	409	412	4	9	-4	0	34	5	1	5	510	-479
0	4	6	358	321	4	0	0	357	-324	6	0	4	61	-121	-2	0	10	0	-41	5	1	-5	758	-779	3	1	6	81	-74
0	4	7	136	139	5	0	0	781	-802	7	0	4	132	-174	-1	0	10	305	294	5	2	-5	152	206	4	1	6	71	29
0	4	8	416	-401	6	0	0	156	-142	8	0	4	0	12	1	0	10	502	452	5	3	-5	455	-484	1	1	7	232	223
0	4	9	0	41	7	0	0	139	140	9	0	4	120	-141	1	0	10	168	156	5	4	-5	226	-242	2	1	7	350	335
0	4	10	228	188	8	0	0	172	-184	-13	0	6	0	-53	2	0	10	0	-2	5	5	-5	447	-460	3	1	7	0	-11
0	5	1	28	-67	9	0	0	290	-281	-12	0	6	0	-6	3	0	10	0	22	5	6	-5	215	239	-2	1	8	36	75
0	5	2	193	-184	10	0	0	155	179	-11	0	6	0	-8	-9	0	12	203	215	5	7	-5	270	-286	-1	1	8	0	42
0	5	3	337	-331	11	0	0	0	-19	-10	0	6	376	-371	-8	0	12	66	96	5	8	-5	147	-161	1	1	8	127	102
0	5	4	205	-220	12	0	0	217	-252	-9	0	6	293	-307	-7	0	12	148	-179	5	9	-5	107	-144	2	1	8	55	5
0	5	5	505	485	-12	0	2	100	143	-8	0	6	391	-383	-6	0	12	209	-229	6	1	-6	92	-64	-2	1	9	193	-194
0	5	6	161	-169	-11	0	2	145	147	-7	0	6	237	-289	-5	0	12	215	-246	6	2	-6	79	-77	-1	1	9	126	-158
0	5	7	70	-92	-10	0	2	315	-369	-6	0	6	295	294	-4	0	12	234	-254	6	3	-6	0	-22					

independent reflections (obtained by use of the S1 sample) was initiated with the heavy-atom positions from the X-ray study⁴⁾ and the deuteron positions postulated just above. In the early stage of the refinement, the occupancy factors of the deuteron positions were fixed at values of 1/3, 2/3, 1/3, 2/3, 1/3, 2/3, and 1.0 for D(1), D(2), ..., D(7) in the same order, according to the suggestion from the DMR study.^{2,3)} After the stage of $R=0.121$, several kinds of full-matrix least-squares refinements were carried out under appropriate constraints, because of the occupancy factors strongly correlate with the temperature factors; these were labeled A, B, C, D, and E as follows.

Refinement A: All the occupancy and temperature factors for the deuteron positions were refined at the same time with no constraint.

Refinement B: The sum of the occupancy factors of the two deuteron positions in each H-bond was fixed at unity.

Refinement C: The occupancy and temperature factors of deuteron were refined alternately every four cycles. This procedure yielded the lowest R_0 (R for non-zero reflections), the minimum standard deviation of observation, and the uniform temperature factors.

Refinement D: The occupancy and temperature factors were varied in alternate cycles. All the occupancy factors were adjusted after every cycle of their refinement

TABLE 5. FINAL POSITIONAL PARAMETERS ($10^4 x_j$), THERMAL PARAMETERS ($10^3 B/\text{\AA}^2$), AND SITE OCCUPANCY FACTORS (W) IN THE HIGH-TEMPERATURE PHASE AT 297 K

Estimated standard deviations are given in parentheses.

The isotropic temperature factors are of the form: $T = \exp(-B \sin^2 \theta / \lambda^2)$.

	W	x	y	z	B
Sn	1.0	3756(7)	2591(14)	5353(7)	224(12)
Cl(1)	1.0	2870(5)	4906(11)	6887(5)	277(9)
Cl(2)	1.0	3076(6)	4986(15)	3051(5)	267(8)
O(1)	1.0	1129(17)	1764(13)	4134(12)	263(16)
O(2)	1.0	-665(12)	2042(14)	5978(10)	228(15)
D(1)	0.38(3)	-913(46)	887(33)	5959(35)	301(46)
D(2)	0.66(4)	1084(32)	349(21)	4062(22)	345(27)
D(3)	0.34(3)	-136(26)	2342(41)	5344(24)	264(36)
D(4)	0.70(3)	544(15)	2024(20)	4819(14)	325(21)
D(5)	0.21(3)	-250(44)	2409(51)	6893(38)	195(47)
D(6)	0.79(4)	477(12)	2246(17)	2982(12)	298(20)
D(7)	0.93(4)	-1494(18)	2882(25)	5457(16)	496(27)

TABLE 6. OCCUPANCY(W_j) AND ISOTROPIC TEMPERATURE FACTORS ($B_j/\text{\AA}^2$) IN $\text{SnCl}_2 \cdot 2\text{D}_2\text{O}$ AT 297 K, OBTAINED BY VARIOUS LEAST-SQUARES REFINEMENTS^{a)}

Refinement	A	B	C	D	E
Conditions of least-squares refinement	No constraint	Sum of deuteron occupancies on each H-bond is constrained to unity	Refinements of occupancy and thermal factor for each deuteron position alternate every four cycles	Adjusted in every cycle, as each oxygen atoms has a total of two deuterons (B and W are refined alternately)	Constrained as each H-bond has one deuteron and each oxygen has two deuterons ($B+D$)
W_1	0.38(6)	0.29 [=1.0- W_2]	0.38(3)	0.44(4)	0.57 [= $W_4 + W_6 - 1.0$]
W_2	0.64(6)	0.71(5)	0.66(4)	0.60(3)	0.43 [=2.0- $W_4 - W_6$]
W_3	0.32(6)	0.25 [=1.0- W_4]	0.34(3)	0.36(3)	0.27 [=1.0- W_4]
W_4	0.65(6)	0.75(5)	0.70(3)	0.65(3)	0.73(5)
W_5	0.12(4)	0.18 [=1.0- W_6]	0.21(3)	0.22(3)	0.16 [=1.0- W_6]
W_6	0.81(6)	0.82(4)	0.79(4)	0.75(4)	0.84(5)
W_7	1.01(8)	1.0	0.93(4)	0.98(5)	1.0
B_1	2.7(9)	1.7(4)	3.0(5)	4.6(6)	6.0(6)
B_2	3.3(5)	3.8(4)	3.5(3)	2.9(3)	1.5(3)
B_3	2.8(8)	1.7(4)	2.6(4)	3.0(4)	2.1(4)
B_4	2.9(4)	3.5(3)	3.3(2)	3.0(2)	3.4(4)
B_5	0.5(12)	1.5(5)	2.0(5)	2.3(5)	1.3(6)
B_6	2.7(3)	3.2(3)	3.0(2)	2.9(2)	3.3(3)
B_7	5.1(5)	5.3(3)	5.0(3)	5.3(3)	5.3(3)
$W_1 + W_2$	1.02(9)	1.0	1.04(5)	1.04(5)	1.0
$W_3 + W_4$	0.97(9)	1.0	1.04(5)	1.01(5)	1.0
$W_5 + W_6$	0.93(9)	1.0	1.00(5)	0.97(5)	1.0
$W_1 + W_3 + W_5 + W_7$	1.83(12)	1.72(8)	1.86(7)	2.0	2.0
$W_2 + W_4 + W_6$	2.10(10)	2.28(9)	2.15(6)	2.0	2.0
Total of W_j	3.93(16)	4.0	4.01(9)	4.0	4.0
R_0 -value	0.108	0.097	0.096	0.096	0.099
STD of obs. ^{b)}	2.25	1.54	1.51	1.52	1.58
NV ^{c)}	56	52	50	50	51
Overall B	not refined	not refined	refined	refined	not refined

a) E.s.d.'s in parentheses are in units of the last significant digit. b) Standard deviation of observation as defined by $\sqrt{w(F_o - F_c)^2 / (NO - NV)}$ (NO : Number of observations). c) NV : Number of variable parameters.

TABLE 7. POSITIONAL PARAMETERS (10^4x_i) AND THERMAL PARAMETERS ($10^3B_{ij}/\text{\AA}^2$) AT VARIOUS TEMPERATURES^{a)}

Temp (Method)		88 K (N.D.)	209 K (X-Ray)	223 K (X-Ray)	293 K (X-Ray)
Sn	<i>x</i>	3773(3)	3763(1)	3754(1)	3744(1)
	<i>y</i>	2565(4)	2568(1)	2575(1)	2599(1)
	<i>z</i>	5335(3)	5347(1)	5347(1)	5359(1)
	<i>B</i> ₁₁	16(8)	182(2)	198(1)	232(2)
	<i>B</i> ₂₂	54(9)	124(2)	151(1)	204(2)
	<i>B</i> ₃₃	36(7)	168(2)	181(1)	218(2)
	<i>B</i> ₁₂	3(9)	9(2)	10(1)	15(1)
	<i>B</i> ₁₃	23(6)	77(2)	69(1)	79(1)
Cl(1)	<i>x</i>	2830(2)	2841(3)	2849(2)	2864(2)
	<i>y</i>	4899(3)	4899(3)	4907(2)	4915(3)
	<i>z</i>	6836(2)	6857(3)	6859(2)	6874(2)
	<i>B</i> ₁₁	73(6)	270(8)	291(6)	359(8)
	<i>B</i> ₂₂	62(6)	158(7)	191(5)	272(7)
	<i>B</i> ₃₃	53(5)	215(7)	230(5)	278(7)
	<i>B</i> ₁₂	2(7)	-3(6)	-3(4)	-7(6)
	<i>B</i> ₁₃	39(5)	124(6)	121(5)	148(6)
Cl(2)	<i>x</i>	3071(2)	3067(2)	3063(2)	3062(2)
	<i>y</i>	5008(3)	4999(3)	4996(2)	4992(3)
	<i>z</i>	3043(2)	3053(3)	3045(2)	3051(2)
	<i>B</i> ₁₁	50(5)	226(7)	237(5)	277(6)
	<i>B</i> ₂₂	59(6)	148(6)	188(5)	256(6)
	<i>B</i> ₃₃	58(5)	170(7)	200(5)	242(6)
	<i>B</i> ₁₂	-2(6)	-4(6)	-4(4)	-5(5)
	<i>B</i> ₁₃	34(5)	86(6)	81(4)	88(5)
O(1)	<i>x</i>	1096(4)	1091(7)	1091(5)	1095(6)
	<i>y</i>	1685(5)	1713(8)	1741(4)	1757(7)
	<i>z</i>	4156(4)	4148(9)	4139(6)	4129(6)
	<i>B</i> ₁₁	54(9)	212(22)	219(15)	242(19)
	<i>B</i> ₂₂	78(10)	135(20)	176(15)	234(19)
	<i>B</i> ₃₃	41(8)	165(21)	177(14)	217(18)
	<i>B</i> ₁₂	-27(11)	-21(17)	-22(12)	-39(16)
	<i>B</i> ₁₃	26(8)	86(17)	73(12)	78(15)
O(2)	<i>x</i>	-683(4)	-678(7)	-671(5)	-674(6)
	<i>y</i>	2058(5)	2053(8)	2065(5)	2067(8)
	<i>z</i>	5931(4)	5956(10)	5960(7)	5984(7)
	<i>B</i> ₁₁	56(9)	207(22)	229(16)	278(21)
	<i>B</i> ₂₂	62(9)	143(21)	173(15)	250(21)
	<i>B</i> ₃₃	59(9)	246(24)	249(16)	300(22)
	<i>B</i> ₁₂	0(12)	16(18)	24(13)	37(17)
	<i>B</i> ₁₃	35(8)	95(19)	87(14)	92(18)
	<i>B</i> ₂₃	-7(10)	3(18)	-1(13)	2(18)

a) Estimated standard deviations are given in parentheses. The anisotropic thermal factors are given by the same expression as in Table 3.

in such a way that an oxygen atom always has a total of two nearest deuterons to constitute a water molecule.

Refinement E: The strong constraint of so-called ice rules was imposed on the refinement. Since each oxygen has a total of two nearest deuterons, and since each H-bond involves one deuteron, only two occupancy factors, such as D(4)'s and D(6)'s, need to be refined. This refinement converged only slightly, and it was far

from satisfactory (see Table 6).

No positional parameters of any of the atoms differed by more than their associated e.s.d.'s among these refinements. Therefore, only the final F_c , the F_o after the extinction correction, and the final positional parameters in the C refinement are presented in Tables 4 and 5. The occupancy factor, W_j , and the isotropic temperature factor, B_j , for the *j*-th deuteron position are compared in Table 6. The extinction correction described above was made before any refinement, and the weighting scheme used throughout the refinement was

$$w = I_o/I_e, \quad \text{if } I_o > 4I_{\min},$$

$$w = (I_o + I_{\min})/5I_{\min}, \quad \text{if } I_o < 4I_{\min},$$

where I_o and I_e were the integrated intensities before and after the extinction correction respectively, and where I_{\min} was the averaged background intensity. The quantity minimized in all least-squares refinements was $\sum w(|F_o| - |F_c|)^2$.

Structure at 209 and 223 K by X-Ray Diffraction. The procedure used was almost the same as in the previous study.⁴⁾ The structure was refined by a block-diagonal least-squares method, with 1582 and 1589 independent reflections at 209 and 223 K respectively. For comparison, the structure at 293 K was refined again including anomalous dispersion corrections for Sn and Cl. In these calculations, the atomic scattering factors for Sn^{2+} , Cl^- , and O^- and anomalous dispersion corrections, f' and f'' for Sn and Cl were taken from the International Tables for X-Ray Crystallography, Vol. IV.¹⁴⁾ The values of R and R_0 at each temperature are [given as T/K , R , R_0]: 209, 0.053, 0.047; 223, 0.045, 0.038; and 293, 0.045, 0.043. The final positional and thermal parameters at 209, 223, and 293 K are summarized in Table 7, together with those at 88 K obtained from the neutron study. A list of the observed and calculated structure factors at 209 and 223 K has been deposited with the Chemical Society of Japan (Document No. 7723).

Computation. All the computations in this study were made on the NEAC 2200/700 at the Computer Center, Osaka University, using local modifications of the RSFLS, RSSFR-5, HBLS-V, and RSDA-4 in the UNICS program system¹⁵⁾ and the stereoscopic drawing program ORTEP.¹⁶⁾

Results and Discussion

Crystal Structure Except for Hydrogens. The crystal contains two kinds of water molecules. The first, $\text{H}_2\text{O}(1)$, is coordinated to a tin atom to form a trigonal pyramidal dichloroaquatin(II) complex, $\text{SnCl}_2 \cdot \text{OH}_2$, whereas the second, $\text{H}_2\text{O}(2)$, does not. These two are H-bonded to each other to construct a puckered water-layer, which extends along the (100) plane. Tin and Cl atoms form double layers parallel to (100), also. Between these Cl/Sn double layers, the water layer intervenes (Fig. 2).

The Sn-Cl(2) bond length is significantly longer (by 0.06 Å) than Sn-Cl(1). This is consistent with the facts that Cl(2) is close to two Sn atoms of different pyramids

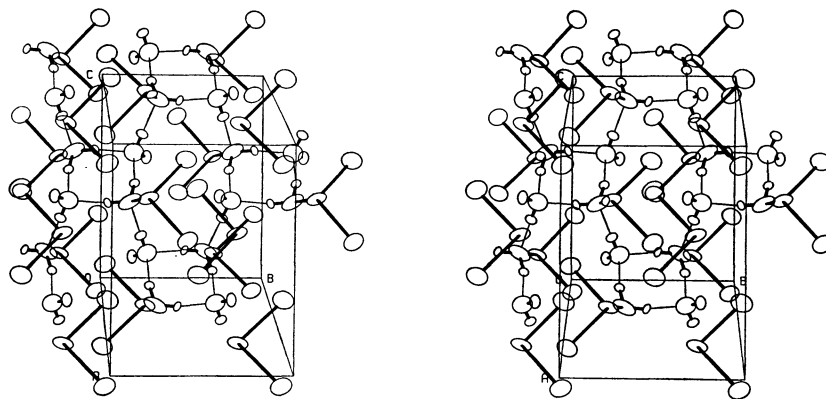


Fig. 2. View of the whole cell in $\text{SnCl}_2 \cdot 2\text{D}_2\text{O}$ determined by ND at 88 K. The c axis is vertical and the b axis is horizontal on the page.

at distances of 3.22 and 3.33 Å, while Cl(1) has two Sn neighbors with much longer separations of 3.41 and 3.65 Å. Such a difference in the nature of the chemical bonds should reflect on the quadrupole resonance (NQR) frequencies of the ^{35}Cl nuclei. Recently Trontelj and Pirnat have detected two NQR frequencies of 8.656 and 8.511 MHz at 300 K.¹⁷ The former can be assigned to Cl(1), and the latter, to Cl(2), because Cl(1) is less ionic than Cl(2) in view of the interatomic distances. Further details with regard to the arrangement of non-hydrogen atoms have already been described in a previous paper.⁴

Hydrogen-ordered Structure at 88 K. The positions and site-occupancy factors of hydrogen atoms are of much interest, because they play a dominant role in the phase transition. The unit cell of the hydrogen-ordered structure is shown in Fig. 2; it was determined by neutron diffraction at 88 K. It was confirmed from these results that the configuration of $\text{D}_2\text{O}(1)$ is Type

H, while that of $\text{D}_2\text{O}(2)$ is Type E, according to the classification of Chidambaram *et al.*¹⁸ In the former, one of the lone pairs of oxygen O(1) is directed toward a tin atom, and the other, toward an H-bond-donor oxygen O(2). On the other hand, two lone pairs of oxygen O(2) are directed toward two H-bond-donor oxygens, O(1) and O(1ⁱⁱⁱ). Thus, the three deuterons, D(2) and D(4) of the coordinated water molecule and D(5) of the non-coordinated one, form three normal O—D···O hydrogen bonds. The remaining one, D(7), of $\text{D}_2\text{O}(2)$ does not participate in any H-bond, but is directed toward one Cl atom rather than two; the separations of D(7)···Cl(1^{iv}) and D(7)···Cl(2^{iv}) are 2.43 and 2.78 Å respectively at 88 K. These ordered, non-centric hydrogen positions are consistent with our PMR and DMR results.^{2,3}

Mognaschi *et al.* have revealed, from their dielectric measurement, that a weak but significant, antiferroelectric interaction develops between the H-bonded

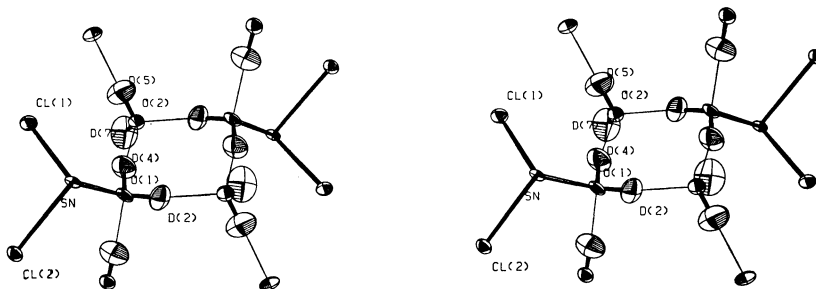


Fig. 3. Stereoscopic drawings of the ordered-arrangement of deuterons with thermal ellipsoids at 50% probability.

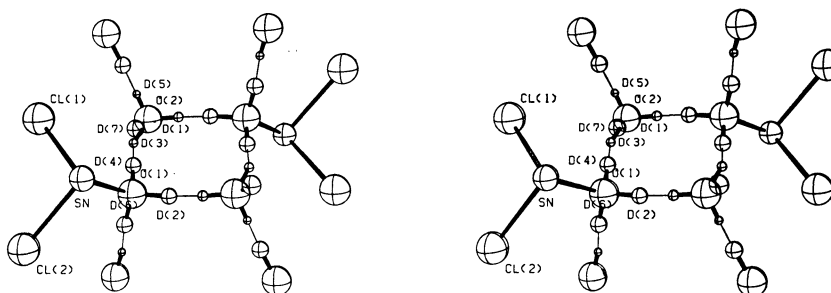


Fig. 4. Stereoscopic view of the disordered-arrangement of deuterons at 297 K. Each occupancy factor given in Table 5 is represented by a size of sphere.

water layers, in addition to the ferroelectric interaction within the layer, as the temperature approaches T_t very closely.⁸⁾ They explained the anomalous behavior of the dielectric constant and of the spin-lattice relaxation rate of protons near T_t in terms of a "critical slowing down" of the electric polarization, as in many ferroelectric and antiferroelectric substances. However, as has been described earlier, our examinations by both X-ray and neutron-diffraction methods showed that no superstructure reflection indicating the doubling of [100] or any lowering of the crystal symmetry appears in the low-temperature phase.

Hydrogen-disordered Structure at 297 K. This compound undergoes the phase transition at 218 K (the deuterated analogue does at 234 K), above which the reorientation rates of both water molecules are high enough to affect the NMR spectra. The deuteron arrangements in the H-bonded layer at 88 and 297 K are compared in Figs. 3 and 4.

In the high-temperature phase, two deuterons of $D_2O(1)$ are distributed among three sites, D(2), D(4), and D(6). In contrast with this, only one deuteron of $D_2O(2)$ is dispersed among the D(1), D(3), and D(5) sites, while the other remains at the fixed position of D(7). This striking feature, together with the DMR results,³⁾ suggests that $D_2O(1)$ and $D_2O(2)$ reorient about Sn–O(1) and O(2)–D(7) bonds respectively, with a nearly three-fold symmetry. If this is the case, the deuteron occupancy factors, W_j , would be 2/3 for D(2), D(4), D(6), and 1/3 for D(1), D(3), D(5). The ND results of the various least-squares refinements given in Table 6 are in fair agreement with the above picture, at least in regard to W_1 , W_2 , W_3 , W_4 , and W_7 .

It is noteworthy, however, that the occupancy factors, W_5 and W_6 , deviate from the expected values by more than three times their e.s.d.'s in all the refinements. This indicates that the H-bond involving D(5) and D(6) is closely associated with the phase transition, as was suggested in a previous paper.¹¹⁾ Salinas and Nagle have calculated, using statistical mechanics, the site occupancy of D(5) as a function of the temperature and have pointed out that its value should be less than 1/3 at high temperatures ($\lim_{T \rightarrow \infty} W_5 = 0.119$).⁹⁾ At room temperature, the theoretical value of W_5 is 0.34, which is larger by 0.1 than the experimental one (0.21 in the C refinement). However, in view of the approximation of the theory and the uncertainty in the experimental occupancy factor, the agreement between these values seems satisfactory. In summary, it may be said that the ND results support the mechanism of the phase transition proposed by Salinas and Nagle.

The results of the least-squares refinements show that each oxygen atom has a total of approximately two deuteron neighbors and that the sum of the two occupancy factors on each H-bond amounts to unity. It can, therefore, be concluded that Bernal and Fowler's ice rules are obeyed in this two-dimensional H-bonded network; hence, scarcely no partial dissociation of water molecules occurs.¹¹⁾

The bond angle of $D_2O(1)$ in the low-temperature phase is typical of a water molecule of crystallization, in spite of a considerably narrow acceptor-angle, O(2)...

TABLE 8. BOND DISTANCES ($l/\text{\AA}$) AND ANGLES ($\theta/^\circ$) DETERMINED BY NEUTRON DIFFRACTION

	88 K	297 K
(a) Water molecules		
O(1)–D(2)	0.973(5)	1.036(18)
O(1)–D(4)	1.004(6)	1.005(22)
O(1)–D(6)		1.011(13)
O(2)–D(1)		0.860(26)
O(2)–D(3)		0.929(32)
O(2)–D(5)	0.952(5)	0.790(35)
O(2)–D(7)	0.955(5)	0.925(19)
Sn–O(1)–D(2)	109.8(3)	106.5(17)
Sn–O(1)–D(4)	113.5(3)	114.2(9)
Sn–O(1)–D(6)		117.0(13)
D(2)–O(1)–D(4)	104.0(5)	102.7(22)
D(2)–O(1)–D(6)		107.5(14)
D(4)–O(1)–D(6)		107.8(16)
D(1)–O(2)–D(3)		115.0(35)
D(1)–O(2)–D(5)		110.1(36)
D(1)–O(2)–D(7)		119.7(27)
D(3)–O(2)–D(5)		113.7(39)
D(3)–O(2)–D(7)		94.6(22)
D(5)–O(2)–D(7)	106.4(5)	102.6(33)
(b) Aquacomplex $\text{SnCl}_2 \cdot \text{OH}_2$		
Sn–Cl(1)	2.510(4)	2.530(11)
Sn–Cl(2)	2.565(4)	2.559(12)
Sn–O(1)	2.318(4)	2.323(16)
Cl(1)–Sn–Cl(2)	86.9(1)	87.8(4)
Cl(1)–Sn–O(1)	83.7(1)	84.0(4)
Cl(2)–Sn–O(1)	87.4(1)	86.4(4)
(c) Hydrogen bonds		
O(1)···O(2 ⁱ) ($=d_{12}$)	2.702(5)	2.781(14)
O(1)···O(2) ($=d_{34}$)	2.718(6)	2.805(20)
O(1)···O(2 ⁱⁱ) ($=d_{56}$)	2.808(4)	2.751(13)
O(2)···O(1)···O(2 ⁱ)	90.2(2)	88.2(5)
O(2)···O(1)···O(2 ⁱⁱ)	109.6(2)	109.4(6)
O(2 ⁱ)···O(1)···O(2 ⁱⁱ)	105.9(1)	105.1(4)
O(1)···O(2)···O(1 ⁱ)	89.8(2)	91.8(5)
O(1)···O(2)···O(1 ⁱⁱⁱ)	113.5(2)	112.1(6)
O(1 ⁱ)···O(2)···O(1 ⁱⁱⁱ)	111.2(2)	111.5(4)
D(1)···O(1)		1.928(24)
D(2)···O(2)	1.737(5)	1.763(19)
D(3)···O(1 ⁱ)		1.949(34)
D(4)···O(2 ⁱ)	1.730(6)	1.816(20)
D(5)···O(1 ⁱⁱⁱ)	1.857(5)	1.972(33)
D(6)···O(2 ⁱⁱ)		1.741(13)
(d) Some interatomic distances		
D(7)···Cl(1 ^{iv})	2.427(5)	2.543(16)
D(7)···Cl(2 ^{iv})	2.777(5)	2.844(20)
O(2)···Cl(1 ^{iv})	3.271(4)	3.364(18)
O(2)···Cl(2 ^{iv})	3.420(5)	3.487(15)
Sn···Cl(2 ^v)	3.162(4)	3.198(11)
Sn···Cl(1 ⁱⁱⁱ)	3.377(4)	3.384(10)
Sn···Cl(2 ⁱⁱⁱ)	3.310(4)	3.336(11)
Cl(1)···Cl(2 ^v)	3.712(3)	3.761(8)
Symmetry code		
none	x, y, z	iii $x, 1/2-y, 1/2+z$
i	$-x, -y, 1-z$	iv $-x, 1-y, 1-z$
ii	$x, 1/2-y, -1/2+z$	v $1-x, 1-y, 1-z$

$\text{O}(1) \cdots \text{O}(2^{\text{ii}})$ (90.2°). On the other hand, some H-O-H angles in the high-temperature phase deviate from the tetrahedral angle or the typical value of 105° , but these deviations are of no significance, because of the large number of refined parameters relative to the number of the intensity data. Some interatomic distances and angles based on the neutron data at 88 and 297 K are compared in Table 8.

Change in the Crystal Structure with the Temperature.

In order to make clear whether or not the ordering of the hydrogen atoms is accompanied by any displacement of other atoms, especially in the vicinity of the transition point, T_t , the crystal structure was analyzed by means of X-ray diffraction at 209 and 223 K, a little below and above T_t .

The structures obtained at both temperatures were almost the same as those previously determined by X-rays at 293 K and by neutron diffraction at 88 K (Table 7), except, of course, for the hydrogen atoms. Only a slight, but, significant change was found in the H-bonded net work. The $\text{O} \cdots \text{O}$ distances of the three non-equivalent H-bonds vary with the temperature in

complicated ways (Fig. 5). In Fig. 5 the H-bonds are designated as d_{12} , d_{34} , and d_{56} , according to the numbering of the deuterons (or protons) involved; the temperature dependence of an $\text{Sn} \cdots \text{Cl}$ separation between adjacent layers is also included for comparison. It is noteworthy again that the H-bond d_{56} differs from the other two in their features; the former distance decreases with an increase in the temperature, whereas those of the other two increase normally. As the temperature approaches T_t from below, these H-bond distances change drastically; one of them contracts and the others elongate, and then just above T_t all three become nearly equal. As a result, the volume change of the unit cell occurring at T_t is quite small, and the single crystal does not shatter nor become opaque on passing through the phase transition.

Thermal Expansion. The high-resolution heat-capacity measurements by Matsuo *et al.* showed that the phase transition is of a quasi-first-order type.⁷⁾ No hysteresis was detected on the curve of any lattice parameter or of the unit-cell volume near T_t , within ± 0.5 K. The anomaly of the linear and volume expansion-coefficients extends over a much wider temperature range than that of the heat capacity. In particular, the volume expansion-coefficient swings in a complicated manner around the phase transition. Figure 6 shows the results deduced by numeric point-by-point differentiation from the lattice parameters at various temperatures. The remarkable elongation of the a-axis about T_t corresponds to an abrupt expansion of the separation between adjacent double layers of Cl and Sn atoms. The anomalous expansion-coefficient along the c-axis reflects the change in the $d_{34} + d_{56}$ with the temperature. On the other hand, the elongation of d_{12} is partly canceled by the contraction of d_{56} , resulting in a monotonic elongation along the b direction. A steep variation near T_t was also found in the monoclinic β angle.

The line profiles of all ($h00$) reflections checked by X-rays are often broadened in both 2θ - ω and ω scans in the low-temperature phase; their half-widths are more than twice the corresponding ones in the high-temperature phase. They can, however, be sharpened by annealing for 24 h 20 K below T_t .

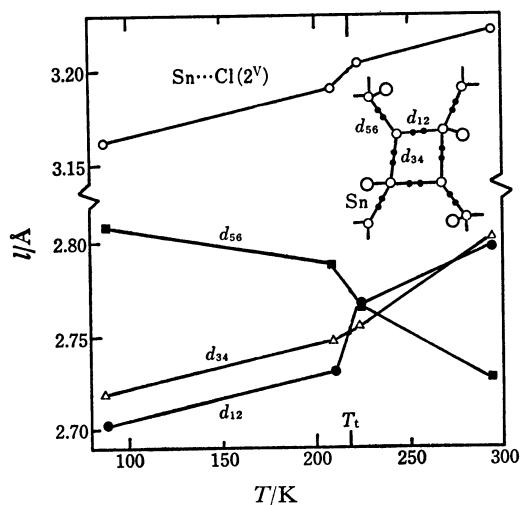


Fig. 5. Plot of three H-bonded $\text{O} \cdots \text{O}$ distances and an $\text{Sn} \cdots \text{O}$ distance against temperature. The results at 88 K come from ND, and the others from X-ray diffraction.

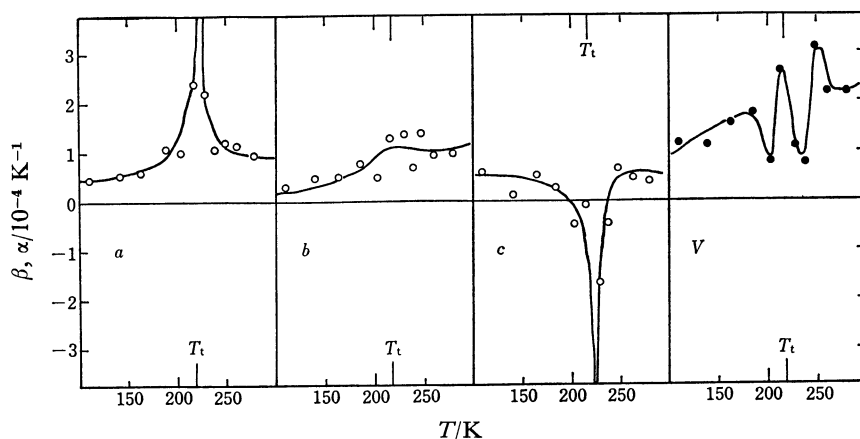


Fig. 6. Temperature dependences of thermal expansion-coefficients. Linear and volume expansion-coefficients are defined as $\beta = 1/l \cdot dl/dT$ and $\alpha = 1/V \cdot dV/dT$, respectively.

The authors are greatly indebted to Professor Iwao Shibuya for his guidance and assistance in this ND work at the Research Reactor Institute, Kyoto University. The authors are also grateful to Professor Emeritus Ryôiti Kiriya for his continued interest and encouragement throughout the present study and to Dr. Takeshi Asai for his careful reading of the manuscript.

References

- 1) H. Kiriya and R. Kiriya, *J. Phys. Soc. Jpn.*, **28**, S114 (1970).
- 2) H. Kiriya, O. Nakamura, and R. Kiriya, *Acta Crystallogr., Sect. A*, **28**, S240 (1972).
- 3) H. Kiriya, O. Nakamura, and R. Kiriya, *Chem. Lett.*, **1976**, 689.
- 4) H. Kiriya, K. Kitahama, O. Nakamura, and R. Kiriya, *Bull. Chem. Soc. Jpn.*, **46**, 1389 (1973).
- 5) H. Morisaki, H. Kiriya, and R. Kiriya, *Chem. Lett.*, **1973**, 1061.
- 6) T. Matsuo, M. Oguni, H. Suga, and S. Seki, *Proc. Jpn. Acad.*, **48**, 237 (1972); T. Matsuo, M. Oguni, H. Suga, and S. Seki, *Bull. Chem. Soc. Jpn.*, **47**, 57 (1974).
- 7) T. Matsuo, M. Tatsumi, H. Suga, and S. Seki, *Solid State Commun.*, **13**, 1829 (1973).
- 8) E. Mognaschi, A. Rigamonti, and L. Menafra, *Phys. Rev. B*, **14**, 2005 (1976).
- 9) S. R. Salinas and J. F. Nagle, *Phys. Rev. B*, **9**, 4920 (1974).
- 10) S. R. Salinas and J. F. Nagle, *J. Phys. Soc. Jpn.*, **41**, 1643 (1976).
- 11) R. Kiriya, H. Kiriya, K. Kitahama, and O. Nakamura, *Chem. Lett.*, **1973**, 1105.
- 12) W. C. Hamilton, *Acta Crystallogr.*, **10**, 629 (1957).
- 13) Neutron Diffraction Commission, *Acta Crystallogr., Sect. A*, **25**, 391 (1969).
- 14) "International Tables for X-Ray Crystallography," Vol. IV, Kynoch Press, Birmingham (1974), pp. 71—98, 148—150.
- 15) T. Sakurai, Ed., "UNICS Program System," Crystallographic Society of Japan (1967).
- 16) C. K. Johnson, ORTEP, Oak Ridge National Laboratory Report ORNL-3794 (1965).
- 17) Z. Trontelj and J. Pirnat, *Proc. 2nd Intern. Symposium on NQR Spectroscopy*, Sept. 3—6 (1973), Viareggio, Italy, ed by A. Colligiani, A. Vallerini Publ., Pisa, pp. 191—205.
- 18) R. Chidambaram, A. Sequeira, and S. Sikka, *J. Chem. Phys.*, **41**, 3616 (1964).
- 19) B. Kamenar and D. Grdenić, *J. Chem. Soc.*, **1961**, 3954.